STEM CELLS TRANSLATIONAL MEDICINE™

TISSUE-SPECIFIC PROGENITOR AND STEM CELLS

High Plasticity of Pediatric Adipose Tissue-Derived Stem Cells: Too Much for Selective Skeletogenic Differentiation?

LEONARDO GUASTI,[a]* WEERAPONG PRASONGCHEAN,[a]* GEORGIOS KLEFTOURIS,[a] SAYANDIP MUKHERJEE,[b] ADRIAN J. THRASHER,[b] NEIL W. BULSTRODE,[c] PATRIZIA FERRETTI[a]

Key Words. Adipose stem cells • Chondrogenesis • Bone • Differentiation • Neural Differentiation

[a]Developmental Biology Unit and [b]Centre for Immunodeficiency, UCL Institute of Child Health, London, United Kingdom; [c]Department of Plastic Surgery, Great Ormond St. Hospital for Children, NHS, London, United Kingdom

*Contributed equally as first authors.

Correspondence: Patrizia Ferretti, Ph.D., Developmental Biology Unit, UCL Institute of Child Health, 30 Guilford Street, London WC1N 1EH, U.K. E-mail: p.ferretti@ucl.ac.uk

Received January 25, 2012; accepted for publication March 20, 2012; first published online in SCTM *EXPRESS* May 3, 2012.

1066-5099/2012/$20.00/0

http://dx.doi.org/10.5966/sctm.2012-0009

ABSTRACT

Stem cells derived from adipose tissue are a potentially important source for autologous cell therapy and disease modeling, given fat tissue accessibility and abundance. Critical to developing standard protocols for therapeutic use is a thorough understanding of their potential, and whether this is consistent among individuals, hence, could be generally inferred. Such information is still lacking, particularly in children. To address these issues, we have used different methods to establish stem cells from adipose tissue (adipose-derived stem cells [ADSCs], adipose explant dedifferentiated stem cells [AEDSCs]) from several pediatric patients and investigated their phenotype and differentiation potential using monolayer and micromass cultures. We have also addressed the overlooked issue of selective induction of cartilage differentiation. ADSCs/AEDSCs from different patients showed a remarkably similar behavior. Pluripotency markers were detected in these cells, consistent with ease of reprogramming to induced pluripotent stem cells. Significantly, most ADSCs expressed markers of tissue-specific commitment/differentiation, including skeletogenic and neural markers, while maintaining a proliferative, undifferentiated morphology. Exposure to chondrogenic, osteogenic, adipogenic, or neurogenic conditions resulted in morphological differentiation and tissue-specific marker upregulation. These findings suggest that the ADSC "lineage-mixed" phenotype underlies their significant plasticity, which is much higher than that of chondroblasts we studied in parallel. Finally, whereas selective ADSC osteogenic differentiation was observed, chondrogenic induction always resulted in both cartilage and bone formation when a commercial chondrogenic medium was used; however, chondrogenic induction with a transforming growth factor β1-containing medium selectively resulted in cartilage formation. This clearly indicates that careful simultaneous assessment of bone and cartilage differentiation is essential when bioengineering stem cell-derived cartilage for clinical intervention. STEM CELLS TRANSLATIONAL MEDICINE *2012;1:384–395*

INTRODUCTION

Stem cell-based therapies for tissue reconstruction present several challenges, including the choice of an appropriate source of cells, the evaluation of risks versus benefits, and the implementation of rigorous protocols. These issues are even more daunting in the case of pediatric patients, particularly those carrying non-life-threatening diseases, where uncertainty about long-term efficacy of cell-based therapies and long-term possible undesirable effects pose several additional ethical issues. Nonetheless, there are several instances where new approaches to tissue reconstruction in children could be highly beneficial and reduce the level of intervention required over time. For example, craniofacial birth defects occur at a relatively high frequency (1 in 1,000 live births), some of them worsen with development, and they often cause severe psychosocial problems in affected children. Management of these defects frequently requires repeated surgical intervention as the patient is growing to ameliorate function and appearance.

A number of craniofacial birth defects involve significant deficits in cartilage, such as dysplastic ears (microtia), airway stenosis, and nasal deformities in facial hypoplasia. Currently, deficits are usually repaired by grafting tissue from another part of the body, involving additional invasive procedures and creating other permanent deficits, as in the reconstruction of outer ear cartilage from costal ribs [1]. The use of bioengineered autologous cartilage could improve clinical management of these patients.

Although cartilage is considered a relatively simple tissue, many issues have to be addressed to achieve cell-based reconstruction of missing/

deformed cartilages, starting from the source of cells. The use of allogeneic cells in children, with consequent need for life-long immunosuppression, would not be desirable. Therefore, the possibility of using autologous chondrogenic cells seeded onto a tailor-made scaffold to bioengineer a tissue that has mechanical properties appropriate for the structure to be repaired and that would not be rejected is of great interest.

Adult adipose-derived stem cells (ADSCs) have generated much interest, given reports suggesting they harbor significant differentiation capability and undergo skeletal (reviewed in [2]), endothelial [3–5], myogenic [6, 7], and even neuronal [8–12] differentiation. They are potentially an ideal cell source, not only because abdominal fat is relatively abundant but also because its harvest is a minimally invasive and much less traumatic procedure than bone marrow harvest, hence, much better suited to young patients. Furthermore, autologous abdominal fat is already used to restore facial contour in children with facial asymmetries (e.g., hemifacial microsomia) [13], with apparently no significant adverse effects. Nonetheless, information on properties and differentiation potential of ADSCs from pediatric patients is still lacking. This needs to be available if we are to consider ADSCs' use for clinical applications in these patients. Furthermore, before using autologous pediatric ADSCs for the management of a patient, it will be crucial to ensure that cells from that patient display a normal behavior; hence, a baseline along which to assess their quality needs to be established.

The aim of this study was to compare, for the first time, ADSCs and adipose explant dedifferentiated stem cells (AEDSCs) from several pediatric patients to assess whether they consistently share the same properties and to extensively characterize them in terms of phenotype, behavior, and differentiation capability under different culture conditions. We also compared their behavior in two- and three-dimensional systems (micromasses), focusing on chondrogenic differentiation. In addition, chondroblast cultures were established from the same patients for direct comparison of their differentiation potential with ADSCs. We show here that pediatric ADSC behavior is comparable across patients, that ADSCs are highly plastic, and that this may be due to the wide range of markers of different cell types they simultaneously express. Furthermore, we show that it is crucial to assess the occurrence of differentiation along more than one lineage under the same culture conditions, as, depending on the medium used, both bone and cartilage are generated, a most undesirable outcome when the aim is to specifically reconstruct one of these tissues.

Materials and Methods

Chemicals

All chemicals were from Sigma-Aldrich (St. Louis, http://www.sigmaaldrich.com), unless otherwise specified.

Culture of Stem Cells from Pediatric Adipose Tissue and Cartilage

Abdominal adipose tissue and costal cartilage were collected from consenting patients under ethical approval from the Camden and Islington Community Local Research Ethics Committee (London, U.K.).

ADSC Cultures

ADSCs were prepared from raw lipoaspirates of 16 young human patients (Fig. 1A; supplemental online Table 1). Lipoaspirates were washed extensively with phosphate-buffered saline (PBS; PAA Laboratories, Linz, Austria, http://www.paa.at) and then incubated with two volumes of 0.05% trypsin/1 mM EDTA (Life Technologies, Rockville, MD, http://www.lifetech.com) in a 37°C shaking incubator for 1 hour. They were then centrifuged at 500*g* for 5 minutes. After removing the supernatant and the floating mature adipocytes, cell pellets were incubated with red blood cell lysis buffer (Roche, Welwyn Garden City, U.K, http://www.roche.co.uk) at room temperature for 5 minutes and then centrifuged again. The so-called stromal vascular fraction containing ADSCs was subsequently grown in a proliferation medium consisting of Dulbecco's modified Eagle's medium (DMEM) high glucose (Life Technologies) supplemented with 10% embryonic stem cell-qualified fetal bovine serum (ES-FBS; Invitrogen, Carlsbad, CA, http://www.invitrogen.com), 2 mM glutamine, and 1% penicillin/streptomycin (all from Life Technologies) at 37°C in a humidified incubator with 5% CO_2. In some experiments, ADSCs were grown in StemPro MSC, a serum-free medium that should support the growth and expansion of human mesenchymal stem cells (Life Technologies). However, as ADSCs grown in this medium died within 2 weeks after an initial increase in proliferative activity, in all studies reported here, the ES-FBS-containing proliferation medium was used.

AEDSC Cultures

After the initial PBS washes, small fragments of human lipoaspirates were plated in six-well plates, and only a small volume of proliferation medium was added to avoid floating. When the cells that had migrated out of the explant reached confluence, the explants were removed, and the cells were cultured and passaged in a proliferation medium as the ADSCs were. We named these explant-derived cells "adipose explant dedifferentiated stem cells."

Costal Chondroblast Culture

Surplus cartilage from patients undergoing autologous costal to ear graft was cut into approximately 2-mm^3 pieces and plated on plastic with proliferation medium. When the cells that had migrated out of the explant were confluent, the explants were removed and cells were expanded in the proliferation medium.

Micromass Cultures

ADSCs and chondroblasts were collected into 1.5-ml Eppendorf tubes (5×10^4 cells per vial), centrifuged at 500*g* for 5 minutes, and incubated at 37°C in 5% CO_2 overnight. The following day, the medium was replaced with control or chondrogenic medium, and cells were fed twice a week for 3 weeks. In each individual experiment, at least three samples per treatment were used. After 3 weeks in culture, either pellets were histologically stained for cartilage and bone differentiation or RNA was extracted.

Generation of Induced Pluripotent Stem Cells from ADSCs

Generation of induced pluripotent stem cells (iPSCs) was carried out according to a previously published protocol [14]. Briefly, human ADSCs were plated on Matrigel in an ADSC proliferation medium and transduced with four single fluorescently tagged lentiviral vectors carrying OCT4, SOX2, KLF4, and c-MYC. The iPSC colonies were maintained in mTesR1 medium (StemCell Technologies, Vancouver, BC, Canada, http://www.stemcell.com).

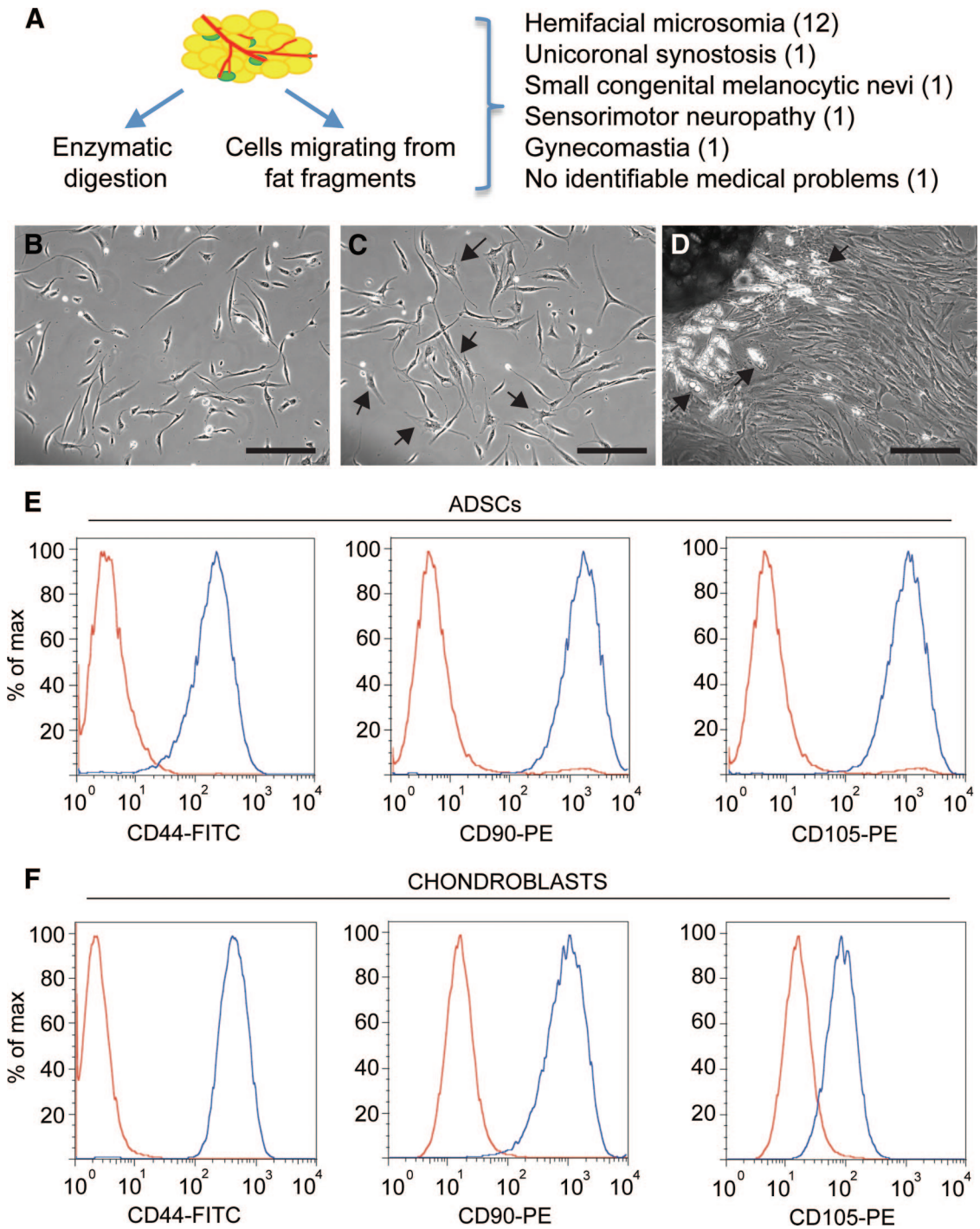

Figure 1. Phase images of ADSC and adipose explant dedifferentiated stem cell cultures. **(A):** Diagram indicating the two approaches used to obtain adipose tissue-derived stem cells from pediatric abdominal fat and summary of donors' conditions (details can be found in supplemental online Table 1). **(B):** ADSC morphology at passage 1. **(C):** ADSC morphology at passage 4. Note the appearance of cells with a more spread out morphology and increased cytoplasm/nucleus ratio (arrows). **(D):** Adipose tissue explant from which cells are migrating. Cells have a multilocular morphology close to the explant (arrows) and become fibroblastic as they migrate away from it. **(E, F):** Expression of the cell surface proteins CD44, CD90, and CD105 assessed by flow cytometry in ADSCs **(E)** and chondroblasts **(F)** from the same patient (red curves: negative controls; blue curves: labeled cells). Scale bar = 200 μm. Abbreviations: ADSC, adipose-derived stem cell; FITC, fluorescein isothiocyanate; max, maximum; PE, phycoerythrin.

Cell Differentiation Protocols and Analysis

Adipogenic Differentiation: Quantification

Three days confluent ADSCs, AEDSCs, and chondroblasts were incubated with a medium containing DMEM 10% ES-FBS, 10 ng/ml insulin, 500 mM 3-isobutyl-1-methylxanthine, 1 mM dexamethasone, and 1 mM rosiglitazone (Molekula, Gillingham, U.K., http://www.molekula.com). After 3 weeks, cells were fixed with 10% formalin, washed with 60% isopropanol for 5 minutes, and stained with Oil Red O (0.25% wt/vol) for 10

minutes. After staining, cells were washed several times with H_2O. For quantification, the dye was extracted with 100% isopropanol for 30 minutes at room temperature, and OD_{495} was determined with a plate reader (Bio-Rad, Hercules, CA, http://www.bio-rad.com). Fold changes were calculated taking untreated controls as reference (value 1).

Chondrogenic Differentiation: Quantification

Confluent cells were incubated in a serum-free StemPro Chondrogenesis Differentiation Kit (Life Technologies; information on the composition of this medium is not available) or with a medium containing DMEM 10% ES-FBS, 0.1 μM dexamethasone, 10 ng/ml transforming growth factor (Tgf) β1 (R&D Systems Inc., Minneapolis, http://www.rndsystems.com), insulin-transferrin-selenium (ITS) (Life Technologies), and 50 μg/ml ascorbate. After 3 weeks, cells were fixed in 4% paraformaldehyde (PFA), rinsed with 0.1 N HCl for 5 minutes and stained with Alcian Blue (1% in 0.1 N HCl). For quantification, the dye was extracted with 6 M guanidine hydrochloride overnight at room temperature, and OD_{595} was determined. Fold changes were calculated, taking untreated controls as reference (value 1). In initial experiments, a medium containing DMEM 10% ES-FBS, 0.1 μM dexamethasone, 10 ng/ml Tgfβ3 (Source BioScience, Nottingham, U.K., http://www.sourcebioscience.com), 10 ng/ml bone morphogenetic protein 6 (BMP6) (Peprotech, Rocky Hill, NJ, http://www.peprotech.com), ITS, and 50 μg/ml ascorbate was also used.

Osteogenic Differentiation: Quantification

Confluent cells were incubated in a medium containing DMEM 10% ES-FBS, 0.1 μM dexamethasone, 100 μg/ml ascorbate, and 10 mM β-glycerophosphate. After 3 weeks, cells were fixed in ice-cold 70% ethanol for 1 hour, washed with H_2O, and stained with 1% alizarin red. For quantification, stained cells were incubated with 10% acetic acid for 30 minutes at room temperature, scraped, transferred to 1.5-ml vials, and heated at 85°C for 10 minutes. Debris was eliminated by centrifugation and the OD_{405} of the supernatants determined. Fold changes were calculated, taking untreated controls as reference (value 1).

Neural Differentiation

The proliferation medium was removed from confluent cultures and replaced with a medium known to promote neural differentiation [9] (DMEM, 10 μM forskolin, 5 mM KCl, 2 mM valproic acid, 1 μM hydrocortisone, 5 μg/ml insulin). In all cases, during differentiation, media were changed twice a week with freshly prepared ones.

Flow Cytometry

ADSCs and chondroblasts (10^6 cells) were fixed in 4% PFA and labeled with 10 μl of either mouse anti-human CD44-fluorescein isothiocyanate (BD Biosciences, San Diego, http://www.bdbiosciences.com), mouse anti-human CD90-phycoerythrin (PE) (Thy; BioLegend, Cambridge, U.K., http://www.biolegend.com/uk), or mouse anti-human CD105-PE (SouthernBiotech) in PBS, 1% fetal calf serum, and 1% bovine serum albumin (BSA). After two washes in PBS/1% BSA, cells were analyzed with a CyAn ADP (Beckman Coulter, Fullerton, CA, http://www.beckmancoulter.com) and histograms created using FlowJo software (Tree Star, Ashland, OR, http://www.treestar.com).

Immunocytochemistry and Immunohistochemistry

Immunocytochemistry was performed as previously described [15] following fixation with 4% PFA in PBS and permeabilization/blocking in 3% BSA, 10% FBS, and 0.2% Triton X-100 in PBS. Cells were incubated with primary antibodies either overnight at 4°C or for 3 hours at room temperature and with secondary antibodies for 1 hour at room temperature. The primary and secondary antibodies used are listed in supplemental online Table 2. Immunostaining of iPSCs, costal cartilage, and some ADSCs was performed using Vectastain ABC kits (Vector Laboratories, Burlingame, CA, http://www.vectorlabs.com). Pictures were acquired with an Axiophot 2 (Carl Zeiss, Jena, Germany, http://www.zeiss.com) with a Hamamatsu ORCA-ER digital camera (Hamamatsu Corp., Bridgewater, NJ, http://www.hamamatsu.com) or an Axiovert 135 (Zeiss) with a ProgRes C14 digital camera using Openlab or Volocity software (PerkinElmer Life and Analytical Sciences, Boston, http://www.perkinelmer.com). To assess the percentage of positive cells, at least 500 cells per coverslips were randomly imaged and analyzed. The same protocol was used to stain 12-μm-thick cryostat sections of human costal cartilage for collagen II (COLII).

Reverse Transcription-Polymerase Chain Reaction and Quantitative Real-Time Polymerase Chain Reaction

RNA was extracted from cells and micromass cultures using Trizol (Life Technologies) according to the manufacturer's protocol. RNA was treated with DNaseI and then phenol-extracted and ethanol-precipitated. One microgram of RNA was then retrotranscribed with Moloney murine leukemia virus reverse transcriptase (Promega, Madison, WI, http://www.promega.com). cDNA was amplified using GoTaq (Promega), using primers and conditions reported in supplemental online Table 3 in a Veriti thermal cycler (Applied Biosystems, Foster City, CA, http://www.appliedbiosystems.com).

mRNA was quantified by real-time quantitative polymerase chain reaction with the Prism 7500 sequence detection system (Applied Biosystems) and the QuantiTect SYBR Green PCR Kit (Qiagen, Hilden, Germany, http://www1.qiagen.com), following the manufacturer's instructions. Primers are shown in supplemental online Table 3. Gene expression data were normalized using *GAPDH* as a reference. Fold changes were calculated taking untreated chondroblasts as reference (value 1).

Statistical Analysis

Statistical significance was evaluated by ANOVA and Student's *t* test, and $p < .05$ was taken to be significant. Data are presented as means $\pm$ SEM. Each experiment was performed on cells from three to seven patients, and samples in each experimental group were $n \geq 3$.

Results

Properties of ADSCs and AEDSCs

Abdominal fat from 16 pediatric patients undergoing reconstructive surgery (Fig. 1A; supplemental online Table 1) was used to generate ADSCs, the stromal cells obtained from enzymatic digestion of abdominal lipoaspirates, and AEDSCs, which were derived from adipose tissue explants. At early passages, ADSCs grown as a monolayer appeared homogeneous, with all cells displaying a fibroblast-like morphology (Fig. 1B). With time in culture, the cell phenotype became more heterogeneous, and some cells with a flattened morphology were observed in these cultures (Fig. 1C).

Table 1. Summary of mRNA and protein expression in ADSCs and AEDSCs

Markers	Antigen	ADSCs		AEDSCs	
		Protein	mRNA	Protein	mRNA
Mesenchymal	Vimentin[a]	All	Yes	All	Yes
	CD44	All	ND	ND	ND
Skeletogenic	RUNX-2	ND	Yes	ND	Yes
	Osterix	ND	Yes	ND	Yes
	Aggrecan	ND	Yes	ND	Yes
	Collagen I	ND	Yes	ND	Yes
	Collagen II	−	−	−	−
	Alkaline phosphatase	ND	−	ND	−
	Osteocalcin	ND	−	ND	−
Adipogenic	Lipoprotein lipase	ND	−	ND	−
	PPARγ	ND	−	ND	−
Neural	Pax6	−	ND	−	ND
	Nestin	+++	Yes	++	Yes
	GFAP	++++	Yes	++++	Yes
	A2B5	All	ND	All	ND
	S100	+	ND	+	ND
	HNK-1	+++	ND	ND	ND
	β3-Tubulin	++++	Yes	++++	Yes
	Doublecortin	−	ND	−	ND
	NF200	++++	Yes	++++	Yes
	NSE	ND	Yes	ND	Yes
	P75NTR	++++	ND	++++	ND
	EAG1	ND	−	ND	−
	Kv 4.3	ND	−	ND	−
Growth factors/receptors	VEGF	All	ND	All	ND
	TGFβ1	All	ND	All	ND
	TGFβ3	All	ND	All	ND
	FLK-1	All	ND	All	ND
Pluripotency	c-Myc	ND	Yes	ND	Yes
	KLF4	ND	Yes	ND	Yes
	Nanog	ND	Yes	ND	Yes
	OCT4	−	Yes	−	Yes
	SOX2	−	ND	−	Yes
	SSEA-1	−	ND	−	ND
	SSEA-3	−	ND	−	ND
	SSEA-4	−	ND	−	ND
	DNMT3B	ND	Yes	ND	Yes
Others	Aq-1	+	ND	ND	ND
	Clusterin	All	ND	All	ND
	Acetylated tubulin	All		All	

Level of expression: −, no expression; +, 1%–25%; ++, 26%–50%; +++, 51%–75%; ++++, 76%–100%; ND, not determined.
[a]Marker also expressed by neural stem cells.
Abbreviations: ADSC, adipose-derived stem cell; AEDSC, adipose explant dedifferentiated stem cell; Aq-1, aquaporin-1; EAG1, ether a-go-go 1; FLK1, fetal liver kinase 1 (VEGFR-2); GFAP, glial fibrillary acid protein; NF200, neurofilament 200; NSE, neuronal specific enolase; p75NTR, p75 neurotrophin receptor; PPARγ, peroxisome proliferator-activated receptor γ; SSEA, stage-specific embryonic antigen; TGF, transforming growth factor; VEGF, vascular endothelial growth factor.

Monolayer cultures were also established from adipose tissue explants. Cells started to migrate from the explant within 2–5 days; these cells initially displayed a multilocular morphology, especially close to the explant, but rapidly lost the characteristic morphology of differentiated cells and acquired a fibroblastic morphology similar to that of ADSCs (Fig. 1D), as also shown by time-lapse photography (supplemental online movie; Fig. 1D). We called these cells AEDSCs.

ADSCs expressed the mesenchymal markers CD44 (hyaluronic acid receptor), CD90 (Thy-1), and CD105 (endoglin), as shown by flow cytometry (Fig. 1E). Expression of proteins that are typically considered markers of either differentiating or fully lineage-committed cells was assessed by immunocytochemistry both in ADSCs and AEDSCs (Table 1; Fig. 2). These cells were found to express mesenchymal, neural, and endothelial proteins (Table 1). All cells expressed vimentin, a mesenchymal marker, acetylated tubulin, a microtubule stability marker in primary cilia, β3-tubulin, and neurofilament 200 (NF-200), both neuronal differentiation markers (Fig. 2A, 2E, 2K, 2L) and, to different extents, a number of other proteins, including early (nestin, A2B5) and late (glial fibrillary acid protein [GFAP]) neural markers, Aquaporin-1, an endothelial marker, growth factors and growth factor receptors (Tgfβ1, Tgfβ3, vascular endothelial growth factor, FLK-1, p75NTR), and CD44 (Fig. 2B–2D, 2F–2J, 2M). The same protein expression pattern was observed in AEDSCs (Table 1), whereas no reactivity was observed in negative controls (Fig. 2N–2O). Expression of neural markers in ADSCs was confirmed by reverse transcription-polymerase chain reaction (Table 1; see also Fig. 4). None of the membrane proteins or transcription factors characteristic of human embryonic stem cells tested were

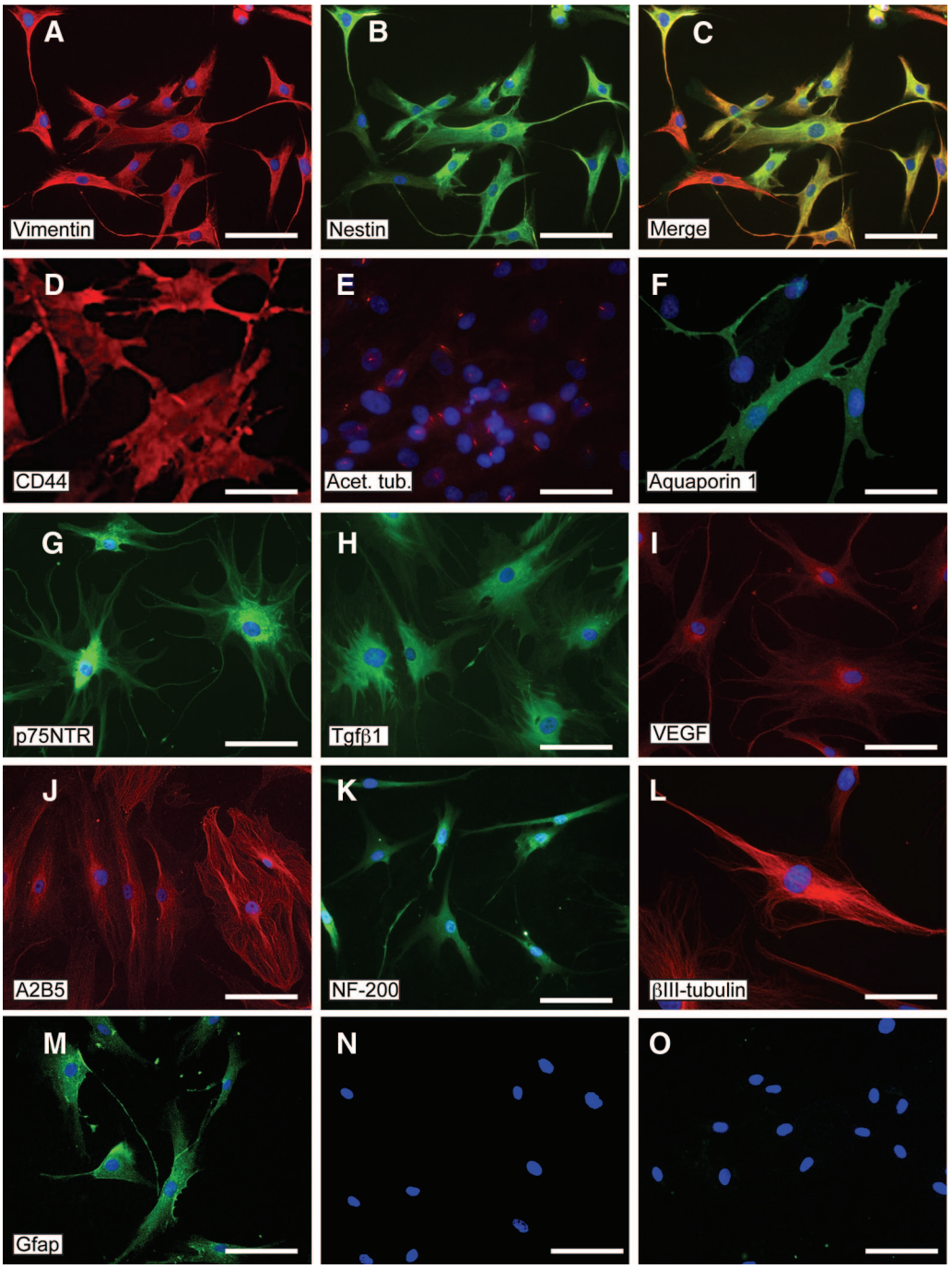

Figure 2. Protein expression in adipose-derived stem cells detected by immunocytochemistry. **(A):** Vimentin. **(B):** Nestin. **(C):** Merged image of **(A)** and **(B)**. **(D):** CD44. **(E):** Acetylated tubulin. **(F):** Aquaporin-1. **(G):** p75NTR. **(H):** Tgfβ1. **(I):** VEGF. **(J):** A2B5. **(K):** NF-200. **(L):** βIII-tubulin. **(M):** Gfap. **(N, O):** Controls for Alexa 568 anti-mouse **(N)** and Alexa 488 anti-rabbit **(O)** immunoglobulin staining (no primary antibody). Nuclei are visualized with 4′,6-diamidino-2-phenylindole (blue). Scale bars = 50 μm **(D, L)** and 100 μm for all other panels. Abbreviations: Gfap, glial fibrillary acidic protein; NF-200, neurofilament-200; Tgfβ1, transforming growth factor β1; VEGF, vascular endothelial growth factor.

detected by immunocytochemistry. In contrast, with the exception of *SOX2*, transcripts for the pluripotency markers *c-MYC, OCT4, NANOG, KLF4,* and *DNMT3B* were detected in ADSCs from all patients tested ($n = 4$; Fig. 3A). Consistent with expression of these factors, ADSCs could be rapidly reprogrammed. Formation of ESC-like colonies (iPSCs) was observed by 10 days after transduction (Fig. 3B–3D), and these cells were positive for the ESC-specific surface antigens, stage-specific embryonic antigen (SSEA) 3 and SSEA4, unlike untransduced ADSCs (Fig. 3E–3G; Table 1).

Differentiation Potential of ADSCs

ADSCs were grown in a variety of media to assess their differentiation potential toward mesodermal and neural lineages under appropriate culture conditions (Fig. 4). When grown in

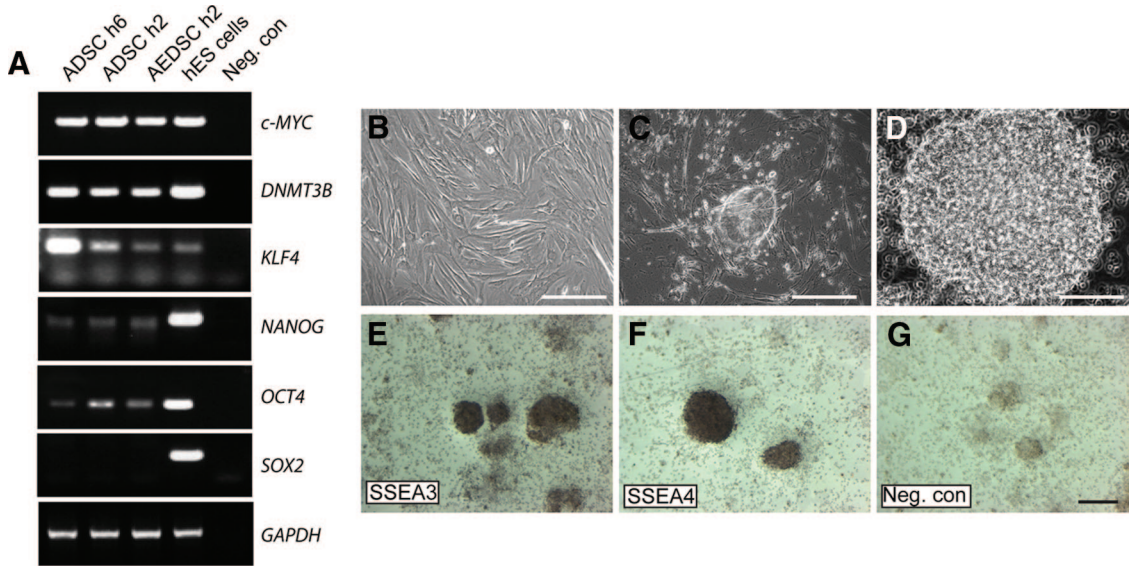

Figure 3. Expression of pluripotency markers in ADSCs and induced pluripotent stem cell generation. **(A):** Expression of pluripotency markers in AEDSCs and ADSCs in different patients (h6 and h2). hES cells were used as positive controls. **(B):** ADSCs plated on Matrigel-coated plates. **(C, D):** Morphological changes and rearrangement of cells 10 days post-lentiviral vector infection **(C)** and after replating **(D)**. **(E, F):** Expression of SSEA3 and SSEA4, respectively. **(G):** Negative control (no primary antibody) for immunocytochemistry. Scale bars = 150 μm **(B, C, E–G)** and 400 μm **(D)**. Abbreviations: ADSC, adipose-derived stem cell; AEDSC, adipose explant dedifferentiated stem cell; hES, human embryonic stem; Neg. con, negative control; SSEA, stage-specific embryonic antigen.

adipogenic differentiation medium, ADSCs expressed peroxisome proliferator-activated receptor γ (*PPAR*γ), the master regulator of adipocyte development, and lipoprotein lipase (*LPL*). Neither of these markers of the adipogenic lineage (Fig. 4A) nor lipid droplets (Oil Red O staining, not shown) were detectable in control cultures. Rapid induction of differentiation in the adipogenic medium was also evident at the morphological level; lipid accumulation was detected by Oil Red O staining as early as 3–4 days after the switch to the adipogenic differentiation medium (not shown) and was extensive by 3 weeks (Fig. 4B). Neither Alcian Blue nor alizarin red staining was observed in cells differentiated in adipogenic medium (not shown).

Under osteogenic differentiation conditions, upregulation of the master regulator of bone cell differentiation Osterix and de novo expression of alkaline phosphatase (*ALP*) and osteocalcin, early and late osteogenic markers, respectively, were detected at the mRNA level (Fig. 4A). Osteogenic differentiation was further supported by alizarin red staining, which detects calcium deposition within the terminally differentiated bone (Fig. 4C).

Different media were compared for their ability to induce chondrogenic differentiation of ADSCs, a Tgfβ1-containing medium, a Tgfβ3/BMP6-containing medium, and a commercially available medium (StemPro Chondrogenesis Differentiation Kit [StemPro-C]). As initial experiments showed fairly similar response of ADSCs to Tgfβ1- and Tgfβ3/BMP6-containing media, only ADSCs' response to the former was studied in detail. After 3 weeks in either Tgfβ1-containing medium (Fig. 4A) or StemPro-C (not shown) de novo mRNA expression of *COLII* transcript, an immature chondrocyte marker was detected. In addition, both the cartilage marker aggrecan and *RUNX2,* the master regulator of chondrocyte hypertrophy as well as of osteoblast commitment, were upregulated. The occurrence of chondrogenic differentiation in both media was supported by Alcian Blue staining and COLII protein expression (Fig. 4D–4G); human costal cartilage was used as positive controls for COLII staining (Fig. 4H, 4I). Chondrogenic differentiation was higher in StemPro-C than in Tgfβ1-containing medium, as confirmed by semiquantitative analysis of Alcian Blue staining (Fig. 4D, 4E, 4J). Cultures differentiated in osteogenic medium did not display any difference in Alcian Blue content, in comparison with untreated controls, consistent with selective bone induction by the osteogenic medium (Fig. 4J). To confirm specificity of skeletogenic differentiation also along the chondrogenic lineage, occurrence of bone differentiation was assessed in parallel with chondrogenic differentiation in cultures grown in StemPro-C and Tgfβ1-containing medium. Whereas hardly any positive alizarin red staining was observed in cultures differentiated in Tgfβ1-containing medium, extensive osteogenic differentiation was found in StemPro-C cultures and was comparable to that observed in the osteogenic medium (insets in Fig. 4D, 4E, 4K). Therefore, StemPro-C is both highly chondrogenic and osteogenic. No Oil Red O staining was observed in cells differentiated in either chondrogenic or osteogenic media (not shown). Mesodermal lineage differentiation was consistently observed in all the lines tested ($n = 7$) and up to at least passage 12, or 5 months in culture. However, the cell doubling time was found to decrease after passage 10.

Phenotypic changes of ADSCs following exposure to a neuronal induction medium were also examined (Fig. 4L–4P). Although several neuronal markers were detected in control ADSCs (Figs. 2, 4L), such as NF-200, neuronal-specific enolase, GFAP, βIII-tubulin, and also a Schwann cell marker, P0, their mRNA levels greatly increased in cells maintained in neurogenic medium. Moreover, mRNAs encoding the voltage-gated potassium channels, *EAG1* (ether a-go-go-1) and *KV 4.3*, were de novo expressed upon neurogenic induction. Significant morphological changes were also observed; the presence of cells with bipolar and multipolar morphology and long projections was consistent with the changes observed at the molecular level (Fig. 4M–4P). These

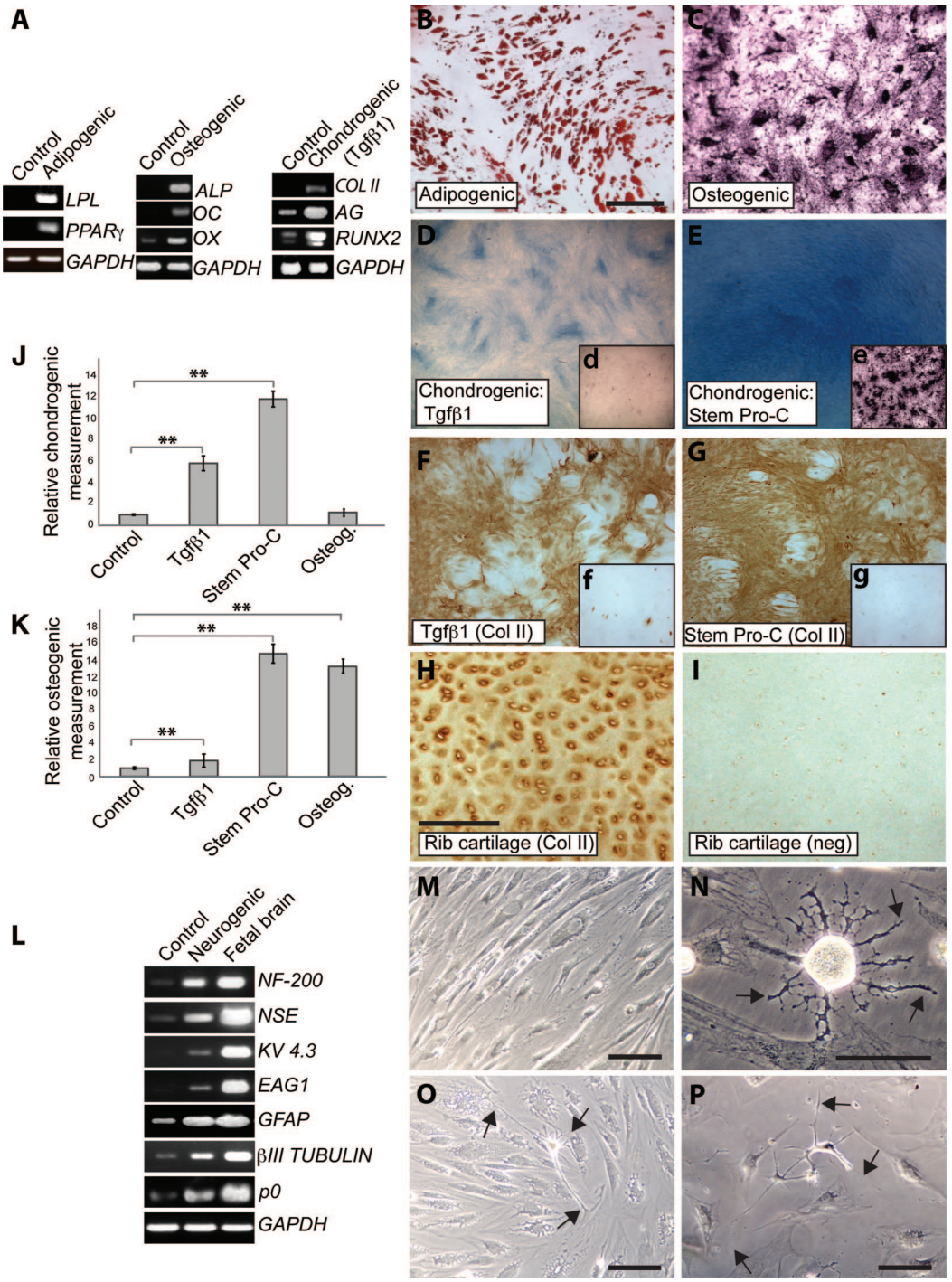

Figure 4. Adipogenic, osteogenic, chondrogenic, and neurogenic differentiation of pediatric adipose-derived stem cells (ADSCs). **(A):** Reverse transcription-polymerase chain reaction showing de novo expression of *LPL* and *PPARγ* upon adipogenic differentiation, de novo expression of *ALP* and *OC* and upregulation of *OX* upon osteogenic differentiation, and de novo expression of *COLII* and upregulation of *RUNX2* and *AG* upon chondrogenic differentiation. **(B):** Cells stained with Oil Red O. **(C):** Cells stained with alizarin red. **(D, E):** Alcian Blue staining of cultures differentiated in either Tgfβ1-containing medium **(C)** or StemPro-C **(D)**. **(Dd, Ee):** Osteogenesis detected by alizarin red staining in StemPro-C **(E)**, but not in Tgfβ1-containing medium **(D)** treated cells. **(F–H)**: COLII staining in ADSCs treated with Tgfβ1-containing medium **(F)** and StemPro-C **(G)** and in a section of human costal cartilage **(H)**. **(Ff):** COLII expression in uninduced ADSCs. **(Gg):** Negative control for COLII staining of ADSCs (no primary antibody). **(I):** Negative control for COLII staining of costal cartilage (no primary antibody). **(J):** Quantification of chondrogenesis (Alcian Blue quantification). Data are expressed as fold differences, taking untreated controls as 1; **, $p < .001$. **(K):** Quantification of osteogenesis (alizarin red quantification). Data are expressed as fold differences, taking untreated controls as 1; **, $p < .001$. **(L):** Expression of neural differentiation markers after 2 weeks in control or neurogenic medium **(B–E)**. Fetal brain cDNA was used as a positive control. **(M):** Phase image of control cells. **(N–P):** Phase images of cells grown in neurogenic medium for 2 weeks. Scale bars = 300 μm **(B)** (**[C–G]** are at the same magnification), 100 μm **(H)** (**[H, I]** are at the same magnification), and 50 μm **(M–P)**. Abbreviations: AG, aggrecan; ALP, alkaline phosphatase; COLII, collagen II; GAPDH, glyceraldehyde 3-phosphate dehydrogenase; GFAP, glial fibrillary acidic protein; LPL, lipoprotein lipase; neg, negative control; NF-200, neurofilament-200; NSE, neuron-specific enolase; OC, osteocalcin; OX, Osterix; PPARγ, peroxisome proliferator-activated receptorγ; Tgfβ1, transforming growth factor β1.

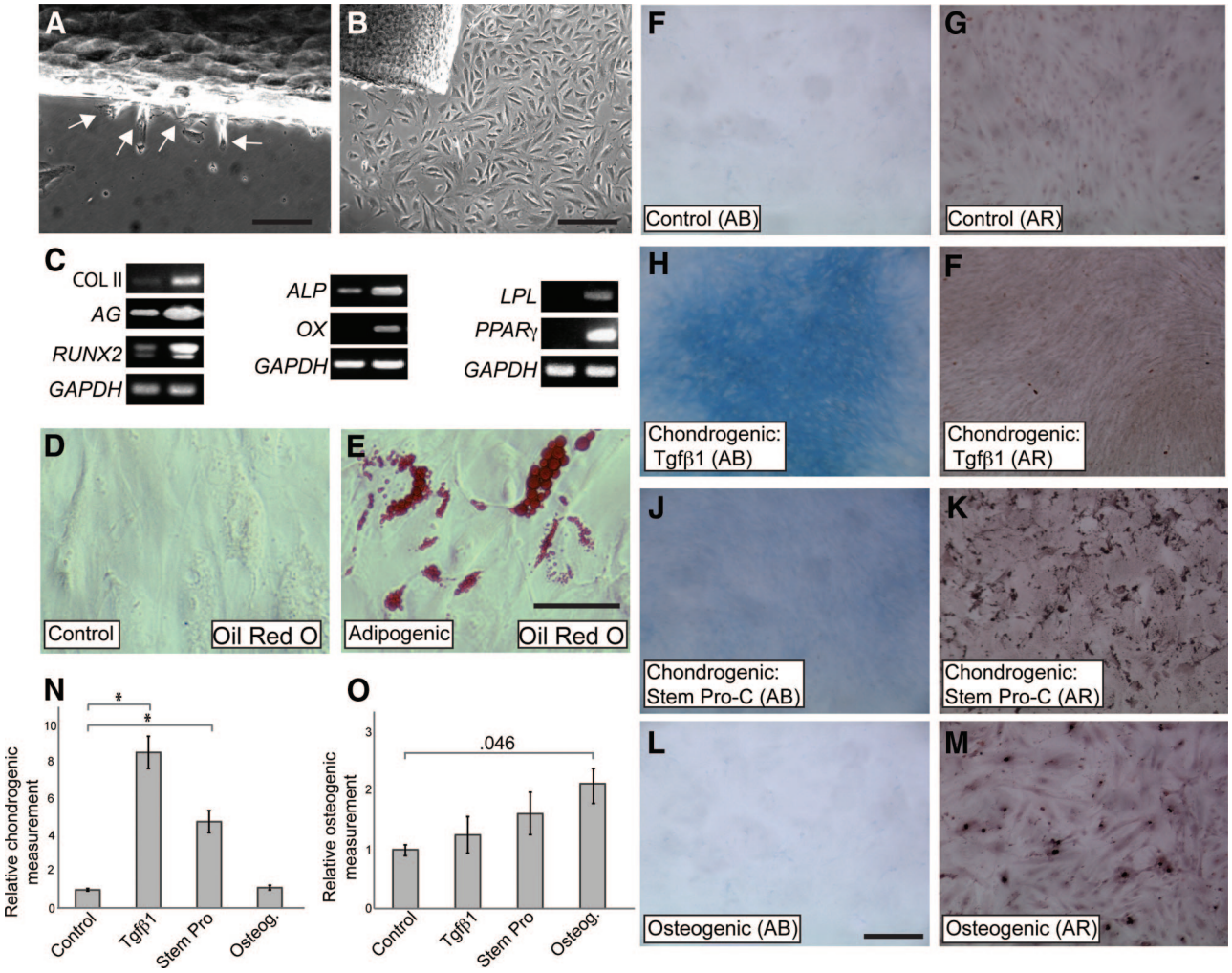

Figure 5. Adipogenic, chondrogenic, and osteogenic differentiation of chondroblasts from costal cartilage. **(A):** Chondroblasts migrating out of the costal cartilage explant at 4 days. **(B):** Chondroblasts migrating out of the explant at 10 days. **(C):** Reverse transcription-polymerase chain reaction showing upregulation of *COLII*, *AG*, and *RUNX2* upon chondrogenic differentiation, upregulation of *ALP* and de novo expression of *OX* upon osteogenic differentiation, and de novo expression of *LPL* and *PPARγ* upon adipogenic differentiation. **(D, E):** Oil Red O staining of chondroblasts treated for 3 weeks with control medium **(D)** or adipogenic medium **(E)**. **(F, G):** Uninduced cells stained with Alcian Blue **(F)** and alizarin red **(G)**. **(H, I):** Tgfβ1-containing medium-treated cells stained with Alcian Blue **(H)** and alizarin red **(I)**. **(J, K):** StemPro-C-treated cells stained with Alcian Blue **(J)** and alizarin red **(K)**. **(L, M):** Osteogenic medium-treated cells stained with Alcian Blue **(L)** and alizarin red **(M)**. **(N):** Quantification of chondrogenesis (Alcian Blue quantification). Data are expressed as fold differences, taking untreated controls as 1; $*$, $p < .002$. **(O):** Quantification of osteogenesis (alizarin red quantification). Data are expressed as fold differences, taking untreated controls as 1. Scale bars = 300 μm **(A, B, L)** (**[F–M]** are at the same magnification) and 50 μm **(E)** (**[D, E]** are at the same magnification). Abbreviations: AB, Alcian Blue; AG, aggrecan; AR, alizarin red; ALP, alkaline phosphatase; COLII, collagen II; GAPDH, glyceraldehyde 3-phosphate dehydrogenase; LPL, lipoprotein lipase; osteog, osteogenic; OX, Osterix; PPARγ, peroxisome proliferator-activated receptor γ; Tgfβ1, transforming growth factor β1.

results suggest that pediatric ADSCs can achieve a neural phenotype.

Comparison of ADSC and Chondroblast Differentiation

Chondroblast cultures were established from pediatric patients' costal cartilage explants to compare their differentiation potential with that of ADSCs. Chondroblast cells migrated out of cartilage explants within 5–7 days after plating and rapidly grew in number (Fig. 5A, 5B). Expression of CD44, CD90, and CD105 in these cultures was similar to that observed in ADSCs (Figs. 1E, 5F). The human chondrogenic precursors could be easily differentiated toward mesenchymal lineages under the same culture conditions used for ADSCs. Some important differences in the response of chondroblasts and ADSCs when induced to differentiate either along the chondrogenic or adipogenic lineage were observed: (a) chondroblasts, but not ADSCs, expressed *COLII* and *ALP* mRNA in control conditions (Fig. 5C); (b) in an adipogenic medium, lipid droplets were observed 3–5 days postinduction in ADSCs but after 3 weeks in chondroblasts (Fig. 5D, 5E), and conversely, in a chondrogenic medium, extracellular matrix deposition could be observed after 3–5 days in chondroblasts but after 2 weeks in ADSCs (not shown); (c) the Tgfβ1-containing medium was more effective than StemPro-C in inducing chondrogenesis in chondroblasts, but it did not induce osteogenesis (Fig. 5F, 5H, 5I, 5J, 5N), whereas the opposite was the case in ADSCs (Fig. 4J); and (d) the StemPro-C medium was not as osteogenic for chondroblasts as it was for ADSCs (Fig. 5G, 5I, 5K, 5M). Osteogenic

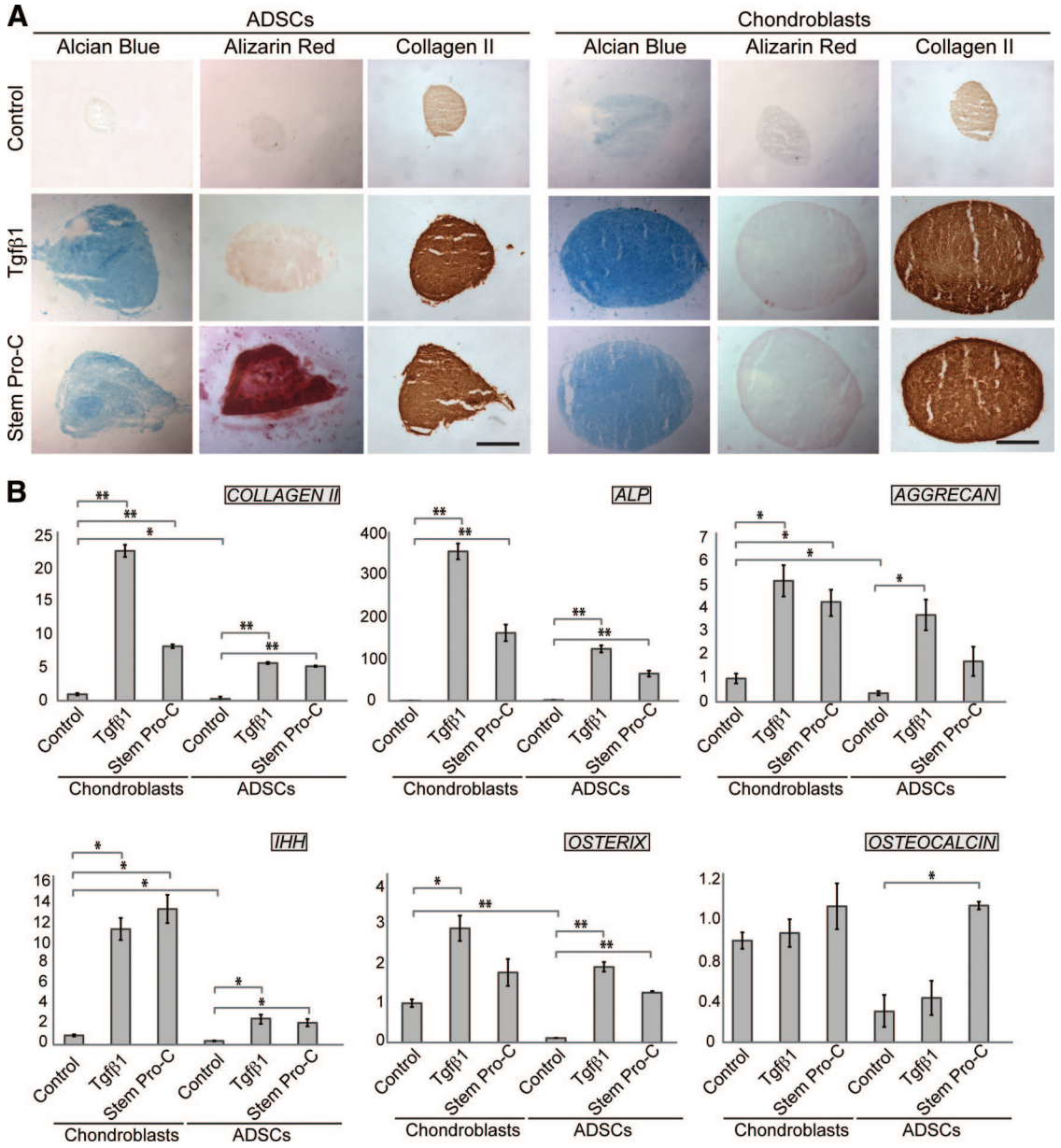

Figure 6. Chondrogenic and osteogenic differentiation of pediatric ADSC and chondroblast micromass cultures in Tgfβ1-containing medium and StemPro-C assessed by histochemistry and Q-PCR. **(A):** Alcian Blue, alizarin red, and collagen II staining of ADSC and chondroblast micromass sections. Scale bars = 250 μm. **(B):** Q-PCR analysis of differentiation markers. The *y*-axes indicate fold changes in relation to untreated chondroblasts. Each experiment was done in triplicate or quadruplicate, and the results shown are representative of those obtained from three patients. Note significant osteocalcin upregulation in ADSC micromass cultures differentiated in StemPro-C; $*$, $p < .05$; $**$, $p < .001$. Abbreviations: ADSC, adipose-derived stem cell; ALP, alkaline phosphatase; IHH, Indian hedgehog; Q-PCR, quantitative polymerase chain reaction; Tgfβ1, transforming growth factor β1.

differentiation of chondroblasts in StemPro-C and osteogenic medium was not significantly different (Fig. 5L, 5M, 5O).

Skeletogenic Differentiation of ADSC in Three-Dimensional Cultures

As the ultimate aim is to use ADSCs for reconstruction of a three-dimensional (3D) tissue, where cell behavior can differ as compared with a monolayer, we investigated the differentiation potential of ADSCs and chondroblasts in a 3D system with micromass cultures (Fig. 6). Micromasses grown in chondrogenic media were analyzed after 3 weeks in culture for chondrogenic and osteogenic differentiation by Alcian Blue, alizarin red, and COLII staining. Alcian Blue staining was present, albeit weak, in chondroblast pellets cultured in control medium (Fig. 6A), suggesting that cell-cell interactions in the 3D system are sufficient to stimulate some proteoglycan synthesis. In contrast, in ADSC micromasses, Alcian blue staining was observed only upon exposure to a chondrogenic medium, either Tgfβ1-containing or StemPro-C medium (Fig. 6A), as observed in the monolayer cultures. Consistent with chondrogenic differentiation, expression of COLII was clearly detected in induced micromasses from both ADSCs and chondroblasts. StemPro-C, but not Tgfβ1, was highly osteogenic in ADSC micromasses, as indicated by alizarin red staining, whereas chondroblast micromasses did not differentiate into bone under any of the chondrogenic conditions tested.

Upregulation of transcripts associated with skeletogenic commitment (*OSTERIX, IHH*) and chondrogenic differentiation (*COLLAGEN II, ALP, AGGRECAN*) was observed in both ADSC and chondroblast micromasses, whereas no significant change in osteocalcin, a bone differentiation marker, was observed in chondroblasts differentiated in either of the chondrogenic media or in ADSCs differentiated in Tgfβ1-containing medium. In contrast, StemPro-C induced a significant osteocalcin mRNA increase in ADSCs (Fig. 6B).

Discussion

We have studied, for the first time, primary cultures of ADSCs and AEDSCs from pediatric patients. Furthermore, we have compared the differentiation potential of ADSCs, AEDSCs, and chondroblasts from costal cartilage generated from the same patients. This is important, as it allows one to rule out that any difference observed in the chondrogenic differentiation ability of these cells might be due to differences in patients' genetic background.

Notwithstanding that the volume of lipoaspirate available from pediatric patients is much smaller (5–10 ml) than that normally used to set up adult cultures (100–300 ml), pediatric ADSCs can be established and expanded to obtain a large number of cells. This makes their potential use for autologous cell therapy a viable option. Significantly, the method we have used to generate AEDSCs, a modification of that previously used to establish dedifferentiated-fat cultures from human [16] and pig [17] lipoaspirates, is simple and allows one to easily generate large numbers of cells from even a smaller amount of starting tissue than required for ADSC preparation. Generation of AEDSCs from the pediatric fat explants appears to occur by direct conversion of adipocytes, as suggested by their rapid loss of lipid droplets and acquisition of a fibroblastic morphology in time-lapse photography studies and by the loss of the differentiated adipocyte markers *LPL* and *PPAR*γ (not shown). Comparison of phenotype and differentiation potential has shown that ADSCs from different patients behave in a remarkably similar fashion both in monolayers and 3D cultures and that ADSCs and AEDSCs display the same phenotype and behavior. Hence, for simplicity, in the following sections we will usually mention only ADSCs.

Pediatric ADSCs are very plastic, as indicated by their reprogramming efficiency and the potential to differentiate along different lineages. As reported for adult ADSCs while our reprogramming studies were in progress [18, 19], pediatric ADSCs can be easily reprogrammed in a feeder-free system using the four Yamanaka's factors, and we have observed colony formation even earlier than reported for adult ADSCs. Whether this may be due to differences in the expression of pluripotency transcription factors between pediatric and adult ADSCs will have to be properly assessed. Nonetheless, it should be noted that whereas *SOX2* is expressed neither in pediatric nor in adult ADSCs, both *NANOG* and *OCT4* transcripts are clearly detected in pediatric ADSCs. In contrast, there is no evidence of *NANOG* expression in adult ADSCs, and low levels of *OCT4* expression have been observed by Sun et al. [18], but not by others [19, 20].

Whereas the relative abundance of fat, its accessibility, and relative ease of ADSC reprogramming can be most useful for establishing models of childhood diseases, the clinical use of iPSCs still poses several safety issues, as, like ESCs, they are tumorigenic. In contrast, ADSCs' wide differentiation potential without a need for full reprogramming to iPSCs makes them a very attractive and safe source of autologous cells for clinical applications in children. Significantly, autologous raw fat transfer is already in use for facial recontouring, for example, in children with hemifacial microsomia [13], boding well for the safety of clinical use of ADSCs.

One important finding reported here is the baseline expression of many different lineage markers in all pediatric ADSC lines examined. As shown by immunocytochemistry, some mesenchymal and neural markers are expressed in all cells and most of them in the majority of cells, suggesting multipotency within the entire population. It is tempting to speculate that coexistence of different lineage markers might underpin the extensive plasticity of ADSCs by maintaining a "ready to go give me directions" state. This could provide ADSCs with the capability of responding to a variety of external stimuli that will then direct differentiation along specific lineages. Some multilineage potential has been proposed also for adult ADSCs [21], but an extensive analysis of lineage markers comparable to that reported here has yet to be carried out in these cells.

We have shown extensive ADSC differentiation into adipocytes, chondrocytes, and osteoblasts, but, with a view to bioengineering cartilage using ADSCs, future studies will need to focus on the mechanical properties of pediatric ADSC-derived cartilage and assess how it compares with chondroblast-derived cartilage. In the case of ADSCs differentiated along the neuronal lineage, more studies are warranted to determine their full extent of differentiation and functional properties and assess whether they could indeed be useful for modeling neural diseases. Upregulation of several neuronal markers, together with de novo expression of potassium channels typical of neurones and the appearance of cells with neuronal morphology, is consistent with the occurrence of neuronal differentiation. It is intriguing, however, that, together with upregulation of neuronal markers, the differentiation conditions used in this study also induce marked upregulation of GFAP, a glial marker, and P0, a Schwann cell marker. Differentiation of adult ADSCs into cells with neuronal and glial phenotype, including Schwann cells, has been previously reported in rats [22, 23], humans [8, 11], and piglets [9], but it has not been assessed whether this occurred simultaneously. Our findings indicate that analysis of only markers specific for a single cell type can be misleading and even dangerous, particularly when differentiation protocols are developed for potential repair/reconstruction of a specific tissue in patients.

This has emerged as a crucial issue also in the case of skeletogenic differentiation. In adipogenic and osteogenic media, ADSCs differentiate accordingly and selectively into adipocytes and bone, respectively, but in chondrogenic media, the emerging picture is more complex. One of the media tested, StemPro-C, was highly osteogenic both in monolayers and 3D cultures. Given that this medium is also highly chondrogenic, it is conceivable that the mixed phenotype it induces results from recapitulation of developmental processes of endochondral ossification and that osteocalcin upregulation reflects the occurrence of chondrocyte hypertrophy and mineralization. In contrast, bone formation in ADSCs is not observed when chondrogenesis is induced using a Tgfβ1-containing medium. Finally, differentiation along the two different skeletogenic lineages does not occur in chondroblasts differentiated in StemPro-C. Whether this reflects the fact that costal cartilage in vivo is not mineralized before early adulthood, a higher commitment to the chondrogenic lineage and/or less plasticity of costal chondroblasts than ADSCs has yet to be established. It should also be noted that a highly plastic cartilage-derived population has been reported to reside

in the perichondrium [24], which was removed from our preparations. Together, these findings show that the Tgfβ1-containing medium provides a good starting point for the optimization of selective cartilage differentiation conditions for potential clinical applications of pediatric ADSCs in cartilage reconstruction.

Conclusion

This study has shown that stem cells derived from pediatric abdominal fat following either enzymatic digestion or explant cultures can be significantly expanded and have comparable properties, making them a potential valuable source of stem cells for autologous cell-based reconstructive surgery in children. This is the first study that focuses on the properties of pediatric ADSCs, compares in parallel ADSCs and chondroblasts from several patients, and scrutinizes differentiation along different lineages in culture conditions supposed to selectively induce a specific cell type. Significantly, this study shows that the advantages of using a highly plastic population that can be directed toward different lineages may be counterbalanced by the fact that differentiation into an undesired tissue type can occur simultaneously under the same culture conditions. Therefore, an important warning message emerging from this study is that the choice of chondrogenic induction medium is of primary importance in reconstructive surgery where only one tissue type must be generated, as, for example, in the case of ear cartilage reconstruction in children with microtia or anotia.

Acknowledgments

This work was supported by NewLife Foundation (to P.F.) and the Office of the Commission on Higher Education of the Royal Thai Government, Thailand (Higher Educational Strategic Scholarship for Frontier Research, to W.P.).

Author Contributions

L.G.: designed experiments, performed experiments, analyzed data, wrote the manuscript; W.P.: designed experiments, performed experiments, analyzed data; G.K.: performed experiments, analyzed data; S.M. and A.J.T.: contributed to iPS derivation; N.W.B., provided clinical samples, clinical background, and critical reading of the manuscript; P.F.: wrote the manuscript, planned research and obtained funding.

Disclosure of Potential Conflicts of Interest

The authors indicate no potential conflicts of interest.

References

1 Tollefson TT. Advances in the treatment of microtia. Curr Opin Otolaryngol Head Neck Surg 2006;14:412–422.

2 Tapp H, Hanley EN, Jr., Patt JC et al. Adipose-derived stem cells: Characterization and current application in orthopaedic tissue repair. Exp Biol Med (Maywood) 2009;234:1–9.

3 Brzoska M, Geiger H, Gauer S et al. Epithelial differentiation of human adipose tissue-derived adult stem cells. Biochem Biophys Res Commun 2005;330:142–150.

4 Zhang P, Moudgill N, Hager E et al. Endothelial differentiation of adipose-derived stem cells from elderly patients with cardiovascular disease. Stem Cells Dev 2011;20:977–988.

5 Cao Y, Sun Z, Liao L et al. Human adipose tissue-derived stem cells differentiate into endothelial cells in vitro and improve postnatal neovascularization in vivo. Biochem Biophys Res Commun 2005;332:370–379.

6 Rodríguez LV, Alfonso Z, Zhang R et al. Clonogenic multipotent stem cells in human adipose tissue differentiate into functional smooth muscle cells. Proc Natl Acad Sci USA 2006;103:12167–12172.

7 Lee JH, Kemp DM. Human adipose-derived stem cells display myogenic potential and perturbed function in hypoxic conditions. Biochem Biophys Res Commun 2006;341:882–888.

8 Jang S, Cho HH, Cho YB et al. Functional neural differentiation of human adipose tissue-derived stem cells using bFGF and forskolin. BMC Cell Biol 2010;11:25.

9 Huang T, He D, Kleiner G et al. Neuron-like differentiation of adipose-derived stem cells from infant piglets in vitro. J Spinal Cord Med 2007;30(suppl 1):S35–S40.

10 Anghileri E, Marconi S, Pignatelli A et al. Neuronal differentiation potential of human adipose-derived mesenchymal stem cells. Stem Cells Dev 2008;17:909–916.

11 Safford KM, Hicok KC, Safford SD et al. Neurogenic differentiation of murine and human adipose-derived stromal cells. Biochem Biophys Res Commun 2002;294:371–379.

12 Erba P, Terenghi G, Kingham PJ. Neural differentiation and therapeutic potential of adipose tissue derived stem cells. Curr Stem Cell Res Ther 2010;5:153–160.

13 Coleman SR. Facial recontouring with lipostructure. Clin Plast Surg 1997;24:347–367.

14 Mukherjee S, Santilli G, Blundell MP et al. Generation of functional neutrophils from a mouse model of X-linked chronic granulomatous disorder using induced pluripotent stem cells. PLoS One 2011;6:e17565.

15 Prasongchean W, Bagni M, Calzarossa C et al. Amniotic fluid stem cells increase embryo survival following injury. Stem Cells Dev 2012;21:675–688.

16 Matsumoto T, Kano K, Kondo D et al. Mature adipocyte-derived dedifferentiated fat cells exhibit multilineage potential. J Cell Physiol 2008;215:210–222.

17 Nobusue H, Kano K. Establishment and characteristics of porcine preadipocyte cell lines derived from mature adipocytes. J Cell Biochem 2010;109:542–552.

18 Sun N, Panetta NJ, Gupta DM et al. Feeder-free derivation of induced pluripotent stem cells from adult human adipose stem cells. Proc Natl Acad Sci USA 2009;106:15720–15725.

19 Sugii S, Kida Y, Kawamura T et al. Human and mouse adipose-derived cells support feeder-independent induction of pluripotent stem cells. Proc Natl Acad Sci USA 2010;107:3558–3563.

20 Aoki T, Ohnishi H, Oda Y et al. Generation of induced pluripotent stem cells from human adipose-derived stem cells without c-MYC. Tissue Eng Part A 2010;16:2197–2206.

21 Guilak F, Lott KE, Awad HA et al. Clonal analysis of the differentiation potential of human adipose-derived adult stem cells. J Cell Physiol 2006;206:229–237.

22 Kingham PJ, Kalbermatten DF, Mahay D et al. Adipose-derived stem cells differentiate into a Schwann cell phenotype and promote neurite outgrowth in vitro. Exp Neurol 2007;207:267–274.

23 Mantovani C, Mahay D, Kingham M et al. Bone marrow- and adipose-derived stem cells show expression of myelin mRNAs and proteins. Regen Med 2010;5:403–410.

24 Kobayashi S, Takebe T, Zheng YW et al. Presence of cartilage stem/progenitor cells in adult mice auricular perichondrium. PLoS One 2011;6:e26393.

See www.StemCellsTM.com for supporting information available online.